Int. J. Electrochem. Sci., 9 **(2014)** 7784 - 7794

International Journal of
ELECTROCHEMICAL
SCIENCE
www.electrochemsci.org

A Facile Synthesis of SiO_2@C@graphene Composites as Anode Material For Lithium Ion Batteries

Yurong Ren[1], *Hengma Wei*[1], *Xiaobing Huang*[2], *Jianning Ding*[1,*]

[1] School of Materials and Engineering, Changzhou University, Changzhou 213164, P. R. China
[2] College of Chemistry and Chemical Engineering, Hunan University of Arts and Science, Changde 415000, P. R. China
[*]E-mail: ryrchem@cczu.edu.cn

Received: 13 September 2014 / *Accepted:* 18 October 2014 / *Published:* 28 October 2014

SiO_2@C@graphene composites were prepared by two-step hydrothermal method and thermal treatment, and then characterized by XRD, FT-IR, Raman, FE-SEM, and TEM. The results demonstrated that SiO_2@C@graphene composites exhibit higher reversible capacity, improved cycling stability, and favorable rate capability compared with bare SiO_2 nanoparticles and SiO_2@C composites. At 50 mA/g, 200 mA/g and 1000 mA/g, the SiO_2@C@graphene composites delivered a discharge capacity of 225 mAh/g, 152 mAh/g, 76 mAh/g, respectively, and after 200 cycles at 50 mA/g, the discharge capacity remained above 250 mAh/g.

Keywords: SiO_2@C@graphene composites; hydrothermal method; thermal treatment; electrochemical performance; Li-ion battery

1. INTRODUCTION

Recently, Graphite has been widely used as anode material in commercialized lithium-ion batteries due to its advantages of long cycle life and low cost [1-3]. Unfortunately, its low lithium-storage capacity has become a huge obstacle to its extensive application, especially in electric vehicles, and electronic devices. Thus far, various different anode materials with high specific capacity have been prepared as new anode candidates, such as Sb-based [4-5], Sn-based [6-7], and Si-based materials [8-9]. Among them, the Si-based materials have attracted the greatest attention, with the highest theoretical specific capacity. However, the drastic volume variation and the poor cycle performance during repeated insertion and extraction of lithium ions have limited its application [10-13]. Several strategies have been proposed to overcome these problems, including preparing nanoparticles, thin films and Si-based composites [14-18].

So far, SiO_2 has been suggested as an alternative anode material for its improved cycling stability in comparsion with Si [19]. Gao et al. claimed that commercial SiO_2 nanoparticles (7 nm in diameter) can react with Li between 0 and 1.0 V (vs. Li/Li^+) with a reversible capacity of 400 mAh/g [20]. After that, SiO_2 with different structures have also been researched as anodes of LIBs, such as film, hollow nanospheres, carbon coated nanoparticles and so on [21-25]. However, the low electronic conductivity of SiO_2 hinders its applications as an electrode material. Grephene is a single-atom-thick sheet-like carbonaceous material with high electronic conductivity and large specific surface area. Therefore, more and more attentions have been paid to graphene owing to its unique properties and potential applications in the areas of energy conversion and storage devices [26-28]. Recently, a double protection method to improve the electrode performance of Si through the use of carbon coating and graphene has been reported [29]. The carbon coated Si nanoparticles and good dispersion of graphene sheets in Si@C nanoparticles realize the double goals of buffering the volume changes and improving the electrical conductivity.

In this paper, we reported the preparation of SiO_2@C@graphene composites by two-step hydrothermal method and thermal treatment. Meanwhile, the electrochemical properties were studied in detail compared with bare SiO_2 nanoparticles and SiO_2@C composites. The result demonstrates that the addition of graphene is an effective way to improve the rate capabilities and stable ability of the SiO_2-based anode materials in LIBs. From a survey of the literature, this is the first report of SiO_2@C@graphene composites used as anode material in LIBs.

2. EXPERIMENTAL

2.1 Preparation of SiO_2 nanoparticles

The SiO_2 nanoparticles were prepared according to a reported method [30]. Briefly, 158 mL absolute ethanol, 7.8 mL ammonia, and 2.8 mL distilled water were introduced in a 250 mL beaker and heated to 50 °C under stirring, then 5.8 mL tetraethyl orthosilicate was added into the solution and stirred at 50 °C for 24 h. SiO_2 nanoparticles were obtained by drying the white solution at 70 °C for 24 h.

2.2 Synthesis of graphene oxide

Graphene oxide (GO) was prepared by the well-known Hummers method [31-32]. In a typical reaction, 2 g of flake graphite, 2 g of sodium nitrate and 96 ml of concentrated sulfuric acid were mixed and stirred for 10 min in a 500 mL round-bottom flask immersed in an ice bath. Then 12 g of potassium permanganate was slowly added to the above solution and stirred for 2 h in the ice bath. After that, the mixture was stirred for 2 h at 35 ^oC, and then 80 mL of deionized water was slowly added to the suspension. Subsequently, the suspension was further treated with 200 mL of deionized water and 15 mL of H_2O_2. After continuously stirring for 30 min, the mixture was washed with water and centrifuged. The graphene oxide was collected and dried at vacuum for 3 days to obtain GO powders.

2.3 Synthesis of SiO_2@C@graphene composites

SiO_2 nanoparticles were coated with a glucose-derived carbon precursor by a simple hydrothermal method. Firstly, SiO_2 ethanol suspension (7.5 mg/ml) and GO aqueous suspension (1 mg/ml) were dispersed by ultrasonic treatment, respectively. Secondly, 1 g of glucose was dissolved in 40 mL deionized water and mixed with SiO_2 dispersion, then the resulting suspension was sealed in a 100-mL Teflon-lined autoclave and retained at 180 ^oC for 10 h. After that, the resultant was centrifuged and washed with water. Thirdly, the collected product was added into 60 ml GO aqueous suspension and sonicated for 1 h to yield a homogeneous suspension, and then sealed in a 100-mL Teflon-lined autoclave and retained at 180 ^oC for 12 h. Finally, the product was centrifuged and washed with water and ethanol, then dried at 60 ^oC for 24 h, and treated at 800 ^oC for 4 h under high-purity nitrogen atmosphere to obtain the SiO_2@C@graphene composites. For comparison, SiO_2@C composites were prepared by the same way without addition of GO.

2.4 Materials Characterization

The crystallographic structure of the samples was characterized using powder X-ray diffraction (XRD, D/max 2500 PC). Compositional analysis for the as-prepared samples was performed with Fourier transform infrared spectroscopy (FT-IR, Avatar 370). The as-received samples were performed by Raman spectrometer (Raman, LabRAM Aramis), The morphologies of the samples were obtained by field emission scanning electron microscopy (FESEM, SUPRA55) and transmission electron microscope (TEM, JEM-2100).

2.5 Electrochemical Measurements

To prepare the working electrodes, 80 wt % of active material, 10 wt % of acetylene black as a conductive material and 10 wt % of sodium carboxymethyl cellulose (CMC) as a binder were dispersed in water solvent to form homogeneous slurry. The slurry was then cast on an copper foil and dried at 100 ℃ for 10 h in a vacuum oven. Finally, CR2032 coin-type cells were assembled in an argon-filled glove box, using lithium foil as the counter electrode, celegard 2400 as the separator, and 1 mol/L $LiPF_6$ dissolved in a mixture of EC, DEC, DMC with a volume ratio of 1:1:1 as the electrolyte. Galvanostatic charge and discharge measurements were performed in a potential range of 0.0-3.0 V at room temperature.

3. RESULTS AND DISCUSSION

Fig.1 shows schematic illustration of the synthesis route for the SiO_2@C@graphene composites. The XRD patterns of GO, SiO_2 nanoparticles, SiO_2@C composites and SiO_2@C@graphene composites are illustrated in Fig.2. As shown in Fig.2 (a), the typical diffraction peak at 10.86°corresponds to the (0 0 2) diffraction line of GO, which consisted with previous reports

[33-34]. The (0 0 2) interlayer distance of GO is calculated to be 0.814 nm, which is significantly higher than 0.337 nm for typical graphite. It might be due to that there are many oxygenic functional groups decorated on both sides and edges of graphene nanosheets.

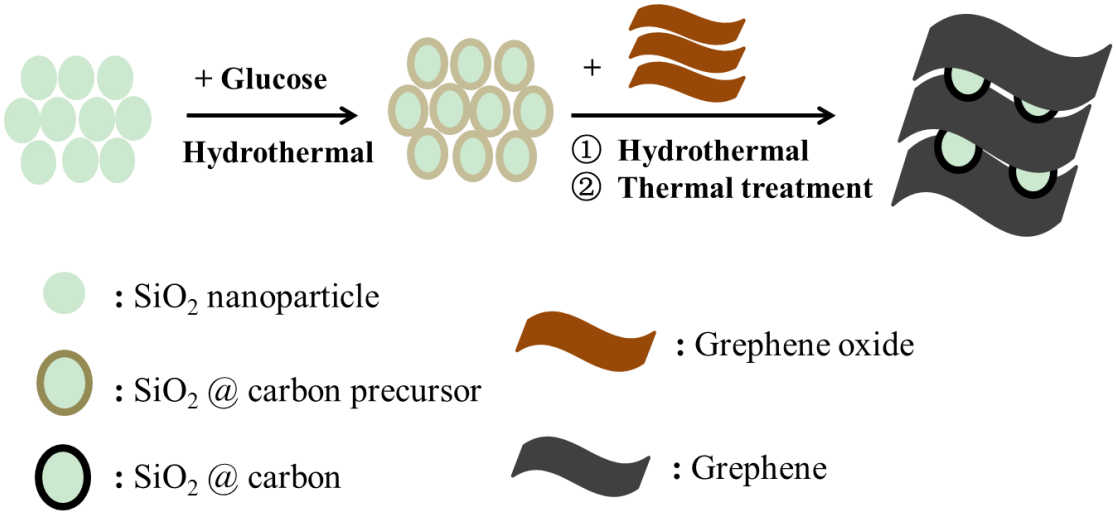

Figure 1. Schematic illustration of the synthesis route for the SiO_2@C@graphene composites.

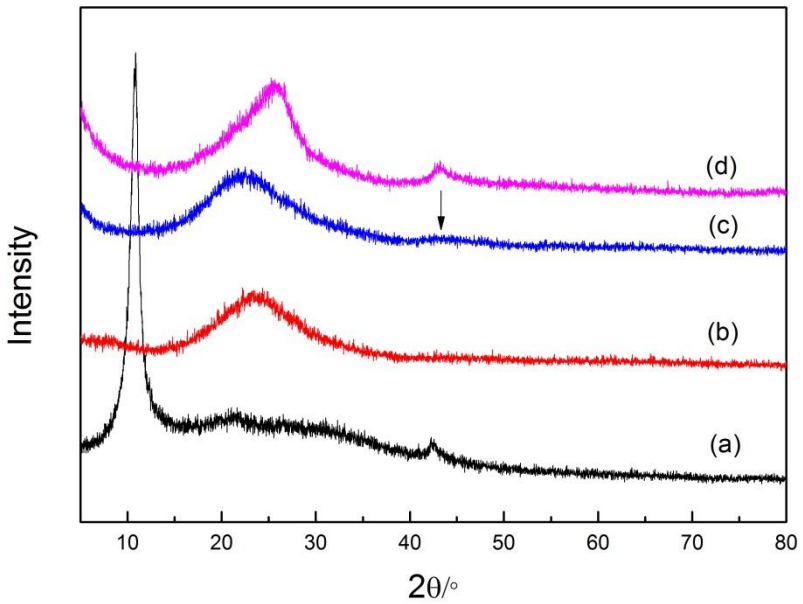

Figure 2. XRD patterns of the as-synthesized (a) GO, (b) SiO_2 nanoparticles, (c) SiO_2@C composites, and (d) SiO_2@C@graphene composites.

Fig.2 (b) and Fig.2 (c) show similar pattern with amorphous SiO_2, except for the weak hump at about 43°in Fig.2 (c) indicates the containing of carbon [35]. The XRD pattern of SiO_2@C@graphene composites in Fig.2 (d) has no any peaks of GO or graphite, and has a little shift to SiO_2@C

composites and bare SiO_2 nanoparticles, which could be caused by graphene and reveals that GO has been reduced by the hydrothermal synthesis and the most graphene nanosheets were separated by SiO_2@C particles [36-37].

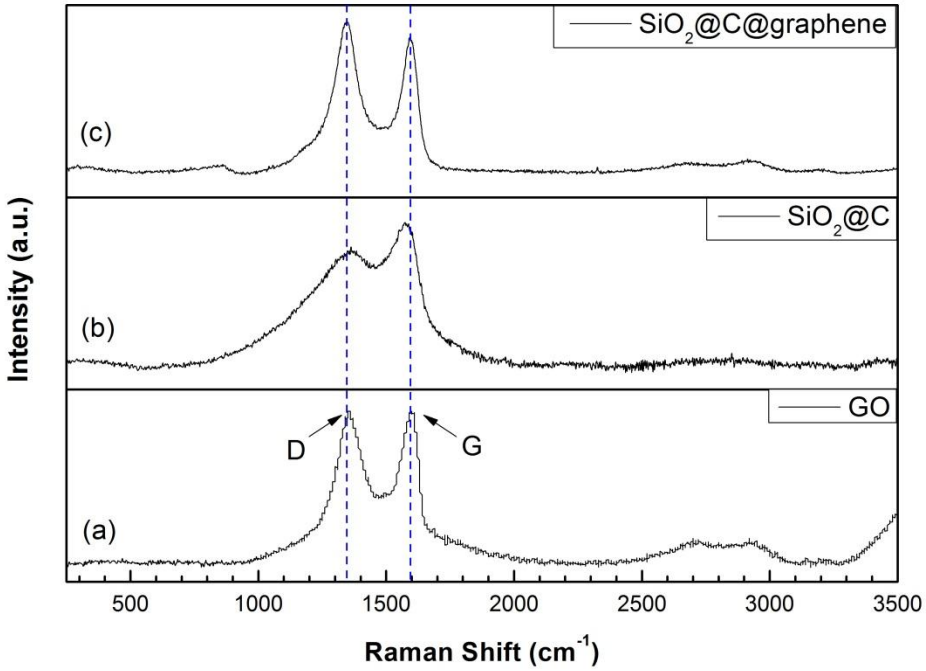

Figure 3. Raman spectra of the as-synthesized (a) GO, (b) SiO_2@C composites, and (c) SiO_2@C@graphene composites.

Fig. 3 presents the Raman spectrum of as-obtained samples. All of the spectrums have two obvious peaks between 1400 cm^{-1} to 1700cm^{-1}, which are assigned to D band and G band of intrinsic feature of carbon materials, respectively [38-39]. Fig.3 (c) demonstrates the peak position of G band and D band shift to lower frequency values compared with Fig.3 (a), which indicated that GO has been reduced to graphene [38]. As well known [40], the intensity ratio of the D and G bands (I_D/I_G) usually shows the ordering degree in the carbon materials. The I_D/I_G of SiO_2@C@graphene composites is higher than that of GO, indicating that the former has a disordered surface. It is consistent with the results from microscopic observations in which the rough morphology of the SiO_2@C@graphene was visible. The Raman results agree well with the XRD results, revealing the synthesis of SiO_2@C@graphene composites through the hydrothermal method and thermal treatment.

Fig.4 presents the FT-IR spectra of as-prepared samples. For SiO_2 nanoparticles in Fig.4 (a), the peaks at 470 cm^{-1}, 798 cm^{-1} and 1107 cm^{-1} are assigned to O-Si-O bending vibration, Si-O-Si symmetric stretching vibration and Si-O-Si unsymmetric stretching vibrations, respectively [41]. Comparing to Fig.4 (a), SiO_2@carbon precursor in Fig.4 (b) shows almost the same peaks at the same positions, except for a broad peak between 3700 and 3000 cm^{-1} corresponds to O-H stretching vibration of hydroxyl or carboxyl, and the weak hump at 960 cm^{-1} corresponds to Si–O stretching vibration of Si–OH [22,32]. For GO in Fig.4 (c), the peaks confirm the presence of the oxygen-containing functional groups in the carbon frameworks. The peaks at 1722, 1402, 1229 and 1068 cm^{-1},

corresponding to C=O stretching of carbonyl groups, C-OH stretching vibrations, C-O vibrations of epoxy groups and C-O vibrations of alkoxy groups, respectively [37].

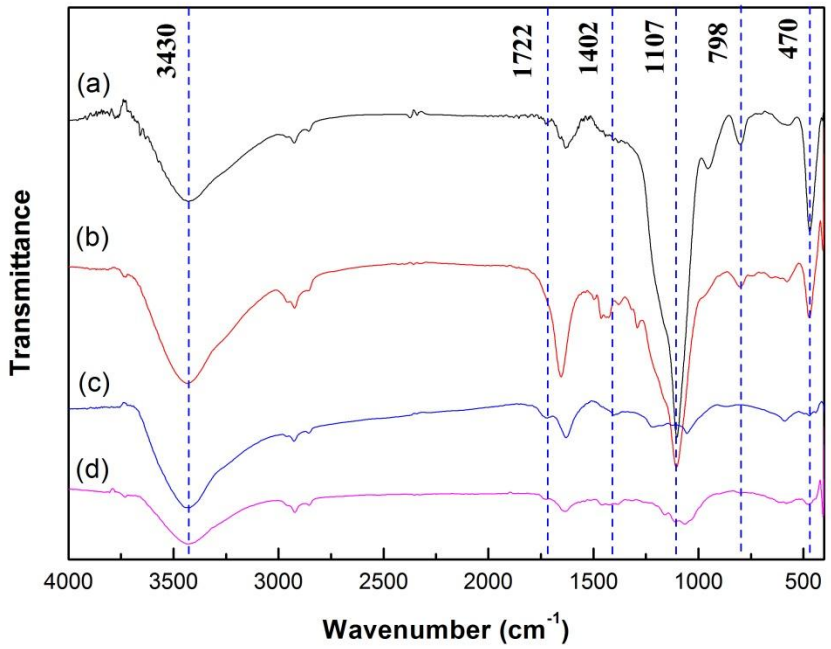

Figure 4. FT-IR spectra of (a) SiO_2 nanoparticles, (b) carbon precursor coated SiO_2 nanoparticles, (c) GO, and SiO_2@C@graphene composites.

Obviously, the carbon precursor coated SiO_2 nanoparticles can be hydrophilic due to the oxygen-containing groups. Therefore, the nanoparticles can be easily dispersed in GO dispersion to form homogeneous suspension, which is benefit to realize the assembly of carbon precursor coated SiO_2 nanoparticles and GO sheets in the hydrothermal step. Moreover, the well-dispersed carbon precursor coated SiO_2 and GO sheets have oxygen-containing functional groups, which can react with each other under hydrothermal way to form a stable structure [32]. In addition, the wide band between 3700 and 3000 cm^{-1} corresponds to O-H stretching vibration in the FT-IR spectrum of SiO_2@C/graphene composite is weaker than carbon precursor coated SiO_2 and GO indicates that some O-H disappeared after hydrothermal process. This result also indicates that the oxygen-containing functional groups on the GO sheets and carbon precursor coated on SiO_2 nanoparticles can react with each other during the hydrothermal process.

The morphology of the as-prepared samples is characterized by field emission-scanning electron microscopy (FESEM) and transmission electron microscopy (TEM). From the SEM and TEM images of SiO_2 (Fig.5a, b) and SiO_2@C (Fig.5c, d), the SiO_2 and SiO_2@C display a quasi-spherical shape with diameters ranging 50-100 nm. It also shows that the SiO_2 and SiO_2@C both have agglomerated and poor dispersion. This result can interpret the poor electrochemical performance of electrodes prepared by bare SiO_2 nanoparticles and SiO_2@C composites, which will be illustrated in Fig.6. From the SEM image of SiO_2@C@graphene composites, we could observe the insertion of SiO_2@C nanoparticles between the interlayers of graphene along the slope. The TEM image of

SiO_2@C@graphene composites reveal that the SiO_2@C nanoparticles are wrapped by the graphene film or embedded in the graphene network.

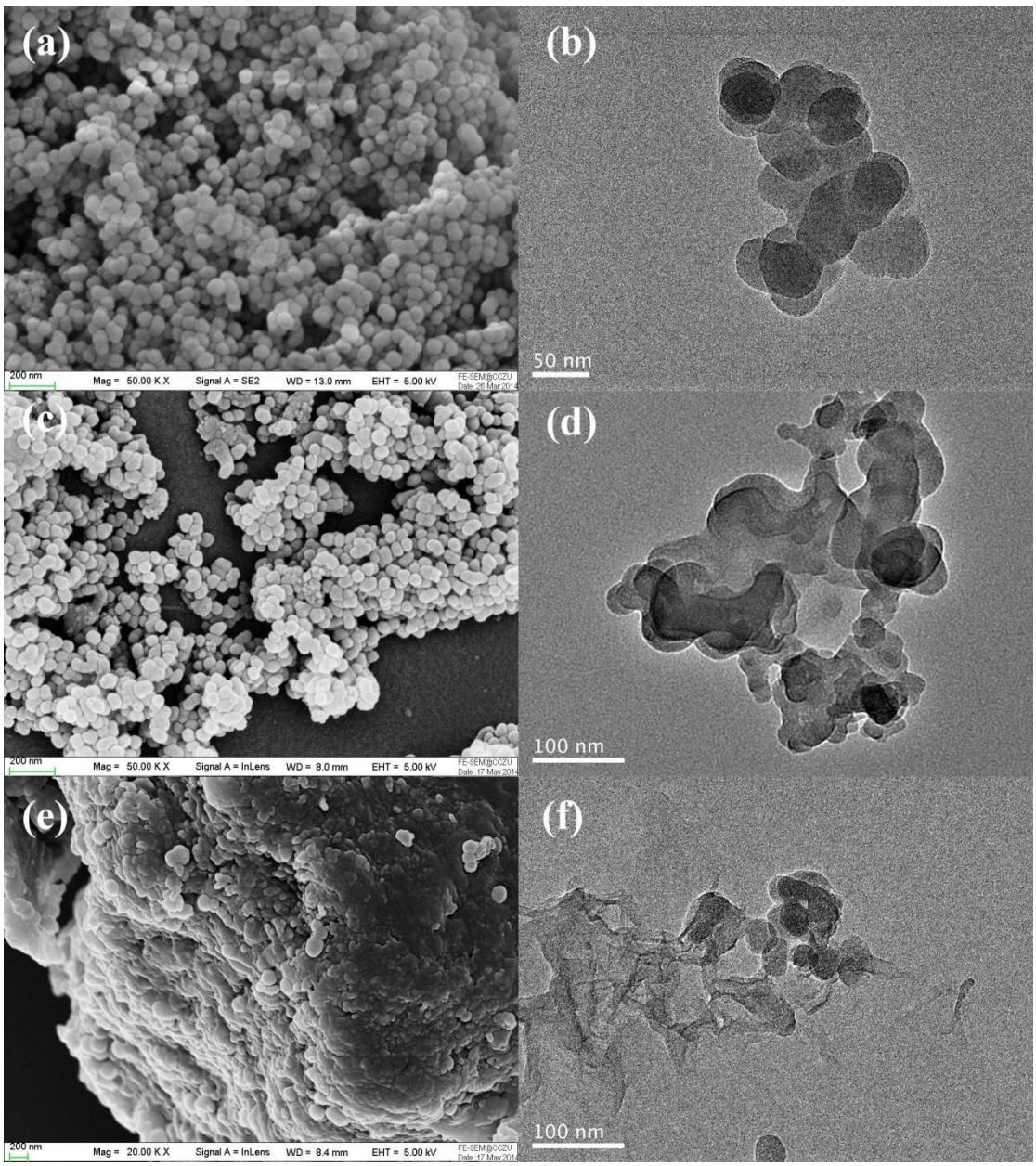

Figure 5. FE-SEM images of (a) SiO_2 nanoparticles, (c) SiO_2@C composites, and (e) SiO_2@C@graphene composites; TEM images of (b) SiO_2 nanoparticles, (d) SiO_2@C composites, and (f) SiO_2@C@graphene composites.

Hence, after hydrothermal process, the SiO_2@C nanoparticles and graphene could be separated by each other. It will be benefit to improve the electrochemical performance of SiO_2@C@graphene composites, and the results are also illustrated in Fig.6.

Fig.6 (a) shows a comparison of the initial charge/discharge cyclic performances for SiO_2 nanoparticles, SiO_2@C composites, and SiO_2@C@graphene composites. The bare SiO_2 nanoparticles

have a very low initial charge and discharge capacity. SiO_2@C composites show better initial cyclic performances than bare SiO_2 nanoparticles, but still leaves much to be desired. In contrast with the bare SiO_2 nanoparticles and SiO_2@C composites, the SiO_2@C/graphene composites show an initial charge capacity of 713.3 mAh/g and charge capacity of 257.4 mAh/g with an initial coulombic efficiency of 36.1%.

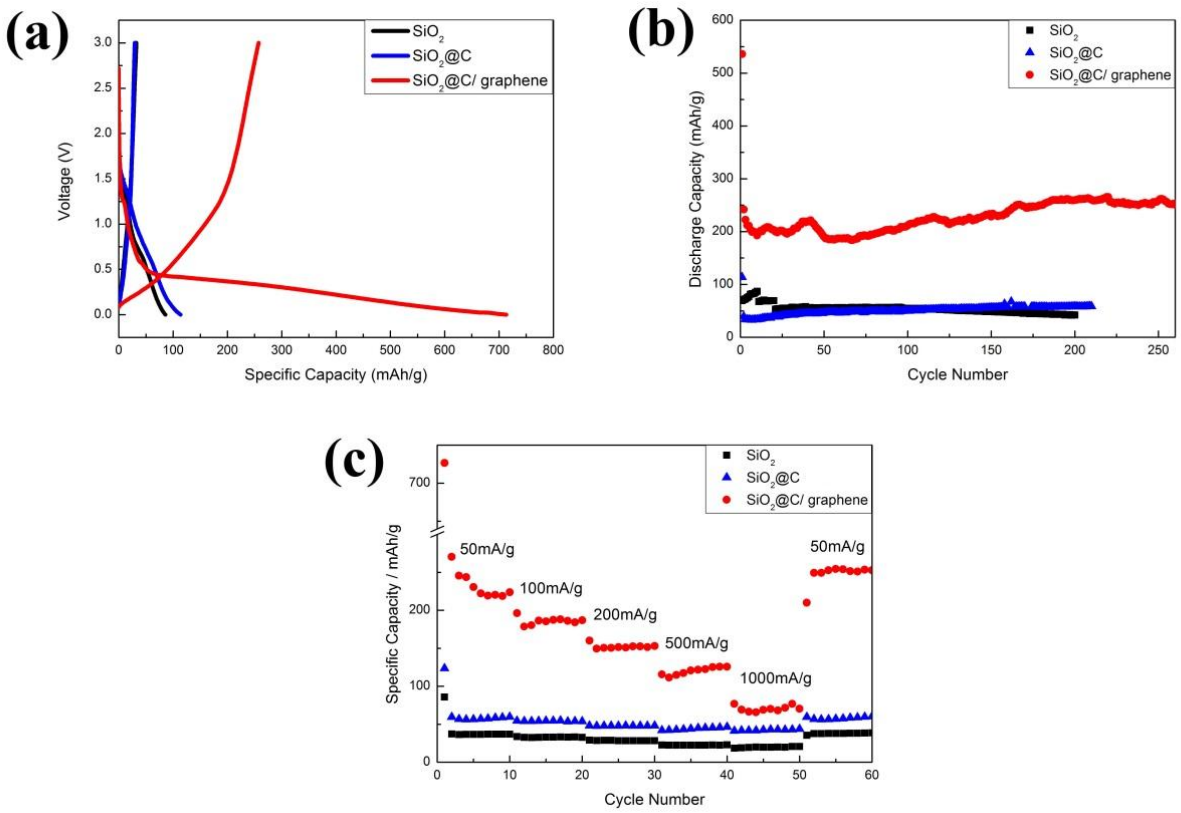

Figure 6. (a) The first discharge/charge curves of bare SiO_2, SiO_2@C composites and SiO_2@C@graphene composites at 50 mA/g; (b) Cycling performances of bare SiO_2, SiO_2@C composites and SiO_2@C@graphene composites at 50 mA/g; (c) Rate capability of bare SiO_2, SiO_2@C composites and SiO_2@C@graphene composites.

The large irreversible capacity during the first cycle can be attributed to the irreversible formation of Li_2O and Li_4SiO_4, which is caused by the reactions of SiO_2 with lithium to form the solid-electrolyte interface (SEI) layer on the electrode surface [23,32]. Comparing to bare SiO_2, SiO_2@C@graphene composites exhibit superior charge capacity and cycling performance, which is attributed to the synergic effect of coated carbon and graphene. According to the previous reports [24,42], graphene nanosheets and carbon shell are active materials for additional Li storage, which is benefit to the reversible specific capacity. Moreover, graphene sheets and carbon shell in the composite not only improve the conductivity of bare SiO_2, but also buffer the volume change during the discharge/charge cycles.

The cycling performance of the SiO_2@C@graphene composites is shown in Fig.6 (b). According to the curves, the SiO_2@C@graphene composites also exhibit better cycle ability with no noticeable decrease in performance over 150 cycles. This result proves that the structure of the composites is very stable. It can be attributed to the following factors. Firstly, the carbon shell can avoid the direct contact between SiO_2 nanoparticles and electrolyte and benefit to the formation of a stable SEI layer. Secondly, the composite consisted of graphene nanosheets and carbon shell can not only act as barriers to suppress the aggregation of SiO_2 nanoparticles, but also prevent the aggregation of the in situ formed nanoparticles (such as Si [23]) during the discharge/charge process.

The rate capability of SiO_2@C@graphene composites is also evaluated and illustrated in Fig.6 (c). When the same cell was tested at various specific currents from 50 to 1000 mA/g, the SiO_2@C@graphene composites exhibit good rate capability. As the specific current increases, the reversible specific capacity declines slowly. At the high specific current of 500 mA/g, the SiO_2@C@graphene composites can keep the upward trend and the capacity increases from 115.7 to125.8 mAh/g. When the specific current is 1000 mA/g, the reversible specific capacity of SiO_2@C@graphene composites shows at a low level, but still higher than the capacity of bare SiO_2 and SiO_2@C composite at 50 mA/g. After 50 cycles at various specific currents from 50 to 1000 mA/g, when the specific current returns to initial 50 mA/g, a reversible specific capacity over 250 mAh/g can be obtained in the 60th cycle, and even higher than the first 10th cycle. The good rate capability of the SiO_2@C@graphene composites can be related to the unique structure of the composite. The network of carbon shell and graphene layer could increase the electronic conductivity and suppress the volume change of the composite during the cyclic process.

4. CONCLUSION

In summary, the SiO_2@C@graphene composites with good electrochemical properties have been prepared by two-step hydrothermal method and thermal treatment. This approach realizes the formation of carbon coatings on the surfaces of SiO_2 nanoparticles and the good dispersion of graphene nanosheets in SiO_2@C matrix simultaneously. The carbon coating in the composite could restrain contact between SiO_2 and electrolyte and buffer volume changes during cycling, leading to favorable coulombic efficiency and improved cycling stability. Meanwhile, the well dispersed graphene sheets could ensure a high electrical conductivity of the composite electrode, resulting in satisfactory capacity, good cycling stability and superior rate capability. The synthesis process of SiO_2@C@graphene composites reported here could also be applied to improve the cyclability and rate capability of other electrode materials with large volume changes and low electrical conductivities.

ACKNOWLEDGEMENT
Financial support from the National Natural Science Foundation of China (51342010 and 5134077), Science and Technology Department of Science and Technology Project in Jiangsu Province （BY2014037-31） are acknowledged, Hunan Provincial Natural Science Foundation of China (13JJ4100 and 12JJ8004).

References

1. J. Dahn, T. Zheng, Y. Liu and J. Xue. *Science*, 1995, 270(), 590-593.
2. C. Doh, C. Park, H. Shin, D. Kim, Y. Chung, S. in, H. Kim and A. Veluchamy. *J. Power Sources* 179(2008), 367-370.
3. L. Su, Z. Zhou and M. Ren.. *Chem. Commun.*, 46(2010), 2590-2592.
4. Y. Li, J.Yang and M. Jiang. *Mater. Lett.*, 62(2008), 2092-2095.
5. Y. Yang, F. Liu, T. Li, Y. Chen, Y. Wu and M. Kong. *Scripta Materialia*, 66(2012), 495-498.
6. Y. Zou, X. Zhou, J. Xie, Q. Liao, B. Huang and J. Yang. *J. Mater. Chem A*, 2(2014), 4524-4527.
7. L. Chen, P. Wu, H. Wang, Y.Ye, B. Xu, G. Cao, Y. Zhou, T. Lu and Y. Yang. *J. Power Sources* 247(2014), 178-183.
8. C.Chan, H. Peng, G.Liu, K. Mcllwrath, X. Zhang, R. Huggins and Y. Cui. *Nature Nanotech.*, 3(2008), 31-35.
9. Y. Liu, Z. Wen, X. Wang, X. Yang, A. Hirano, N. Imanishi and Y. Takeda. *J. Power Sources* 189(2009), 480-484.
10. M. Ge, J. Rong, X.Fang and C. Zhou. *Nano Lett.*, 12(2012), 2318-2323.
11. S. Klankowski, R. Rojeski, B. Cruden, J. Liu, J. Wu and J. Li. *J. Mater. Chem A*, 1(2013), 1055-1064.
12. M.Gauthier, D.Mazouzi, D. Reyter, B.Moreau, D. Guyomard and L. Roué. *Energy Environ. Sci.*, 6(2013), 2145-2155.
13. C. Sun, K. Karki, Z.Jia, H. Liao, Y. Zhang, T. Li, Y. Qi, J. Cumings, G.W. R. and Y. Wang. *ACS Nano*, 7(2013), 2717-2724.
14. H. Kim, M.Seo, M. Park and J.Cho. *Angew. Chem.*, 49(2010), 2146-2149.
15. H. Jung, M. Park, S.Han, H. Lim and S.Joo. *Solid State Commu.*, 125(2003), 387-390.
16. N. Dimov, S. Kugino and M. Yoshio. *Electrochim. Acta*, 48(2003), 1579-1587.
17. Z. Zhang, M. Zhang, Y. Wang, Q. Tan, X. Lv, Z. Zhong, H. Li and F. Su. *Nanoscale*, (12) (2013), 5384-5389.
18. L. Xue, G. Xu, Y. Li, S. Li , K. Fu , Q. Shi and X. Zhang. *ACS Appl. Mater. Inter.*, 5 (2013), 21-25.
19. J. G. Tu, Y. Yuan, P. Zhan, H. D. Jiao, X. D. Wang, H. M. Zhu, S. Q. Jiao. *J. Phys. Chem. C*, 118(2014),7357−7362.
20. B. Gao, S. Sinha, L. Fleming and O.Zhou. *Adv. Mater.*, 11(2001), 816-819.
21. Q. Sun, B. Zhang and Z.W. Fu. *Appl. Surf. Sci.*, 13(2008), 3774-3779.
22. M. Sasidharan, D.Liu, N. Gunawardhana, M. Yoshio and K. Nakashim. *J. Mater. Chem.*, 21 (2011), 13881-13888.
23. Y. Yao, J. Zhang, L.Xue, T. Huang and A. Yu. *J. Power Sources* 196 (2011), 10240-10243.
24. B. Guo, J. Shu, Z. Wang, H. Yang, L. Shi, Y. Liu and L. Chen. *Electrochem. Commun.*, 10 (2008), 1876-1878.
25. M. Li, J. Li, K. Li, Y. Zhao, Y. Zhang, D. Gosselink and P. Chen. *J. Power Sources* 240(2013), 659-666.
26. A. K. Geim. Graphene: Status and Prospects. *Science*, 324 (2009) 1530-1534.
27. P. Wong, H. Tseng, Y. Chen, B. Hwang, L. Chen and K. Chen. *Carbon*, 63(2013), 397-403.
28. G. Zhao, L. Zhang, Y. Meng, N. Zhang and K. Sun. *J. Power Sources* 240(2013), 212-218.
29. H.Li, C. Lu and B. Zhang. *Electrochim. Acta*, 120(2014), 96-101.
30. H. Gong, N. Li and Y. Qian. *Int. Electrochem. Sci.*, 8(2013), 9811-9817.
31. S. Hummers, E. Offeman. *J. Am.Chem. Soc.*, 6 (1958) 1339-1339.
32. P. Lian, J. Wang, D. Cai, L. Ding, Q. Jia and H. Wang. *Electrochim. Acta*, 116(2014), 103-110.
33. C. Nethravathi, M. Rajamathi. *Carbon*, 46 (2008), 1994-1998.
34. J. Chen, L. Yang, S. Fang, Z. Zhang and S. Hirano. *Electrochim. Acta*, 105(2013), 629-634.
35. C. Guo, D.Wang, T. Liu, J. Zhu and X. Lang. *J. Mater. Chem A*, 2 (2014), 3521-3527.

36. Y. Du, G. Zhu, K. Wang, Y. Wang, C. Wang and Y. Xia. *Electrochem. Commun.*, 36(2013), 107-110.
37. X. Zhou, T. Shi. *Appl. Surf. Sci.*, 259(2012), 566-573.
38. H. Xia, Y. Qian, Y. Fu and X. Wang. *Solid State Sci.*, 17(2013), 67-71.
39. D. Wang, M. Gao, H. Pan, J. Wang and Y. Liu. *J. Power Sources* 256(2014), 190-199.
40. J. Ha, S. Park, S. Yu, A. Jin, B. Jang, S. Bong, I. Kim, Y. Sung and Y. Piao. *Nanoscale*, 5(2013), 8647-8655.
41. Y. Sun, L. Zhang, Y. Wang, P. Chen, S. Xin, H. Jiu and J. Liu. *J. Alloy. Comp.*, 586(2014), 441-447.
42. P. Lian, X. Zhu, S. Liang, Z. Li, W. Yang and H. Wang. *Electrochim. Acta*, 55 (2010), 3909-3914.